

Thermodynamics for the Hydrogenation of Dimanganese Decacarbonyl

R. J. Klingler* and J. W. Rathke*

Received August 9, 1991

The equilibrium constant for the hydrogenation of $\text{Mn}_2(\text{CO})_{10}$ in supercritical carbon dioxide has been measured under carbon monoxide and hydrogen at total system pressures of 142–300 atm by in situ ^{55}Mn and ^1H NMR spectroscopy over the temperature range 165–220 °C. The hydrogenation of $\text{Mn}_2(\text{CO})_{10}$ is efficiently promoted by the addition of $\text{Co}_2(\text{CO})_8$ to the system. The rate of $\text{HMn}(\text{CO})_5$ production at 100 °C is increased by 2 orders of magnitude with the addition of 1 equiv of $\text{Co}_2(\text{CO})_8$. The magnitude of this promotional effect has extended the range of temperatures down to 80 °C over which it is feasible to determine the equilibrium constant for $\text{Mn}_2(\text{CO})_{10}$ hydrogenation. van't Hoff plots for the hydrogenation of $\text{Mn}_2(\text{CO})_{10}$ in the presence and absence of the $\text{Co}_2(\text{CO})_8$ promoter were found to yield standard enthalpy and entropy changes that agree to within the statistical error limit of the equilibrium constant measurements. The resultant analysis for the combined data set yields $\Delta H^\circ = 8.7 \pm 0.3$ kcal/mol and $\Delta S^\circ = 8.5 \pm 0.8$ cal/(K·mol) for the hydrogenation of $\text{Mn}_2(\text{CO})_{10}$. The heterobimetallic dimer $\text{Mn}(\text{CO})_5\text{-Co}(\text{CO})_4$ is observed as an additional reaction product in both the ^{55}Mn and the ^{59}Co NMR spectra, within the mixed-metal system. The thermodynamics for the redistribution reaction yielding 2 equiv of $\text{MnCo}(\text{CO})_5$ from the homonuclear dimers, $\text{Mn}_2(\text{CO})_{10}$ and $\text{Co}_2(\text{CO})_8$, was found to be nearly thermal neutral exhibiting $\Delta H^\circ = 0.8 \pm 0.3$ kcal/mol and $\Delta S^\circ = 0.7 \pm 0.8$ cal/(K·mol), respectively.

Introduction

The reductive cleavage of metal–metal-bonded dimers is a general reaction pathway for homolytic hydrogen activation that is central to the function of an entire class of hydrogenation catalysts.¹ In the past, particular attention has been directed toward determining the kinetics, reaction mechanism, and thermodynamics^{2–4} for the dicobalt octacarbonyl system of eq 1,



because it is an industrially used hydroformylation catalyst.⁵ In contrast, the thermodynamics for the analogous manganese system of eq 2 has not been previously determined, despite the prominent role that $\text{HMn}(\text{CO})_5$ has played in studies of olefin hydrogenation by hydrogen atom transfer.⁶



Recently we have described an in situ high-pressure NMR probe⁷ that is ideally suited to investigate^{8a,b} the homolytic hydrogen activation process exemplified by the reaction in eq 1. The present study extends our work with the high-pressure NMR probe to report the equilibrium thermodynamics for the hydrogenation of dimanganese decacarbonyl (eq 2) as measured by in situ ^{55}Mn and ^1H NMR spectroscopy. The direct measurement of the

thermodynamics for the reaction in eq 2 allows an independent comparison to be made between the range of literature values which have been reported for the Mn–Mn bond dissociation energy, BDE, in $\text{Mn}_2(\text{CO})_{10}$ with a recently reported value based on electrochemical and pK_a measurements for the Mn–H BDE in $\text{HMn}(\text{CO})_5$.

Experimental Section

NMR Spectroscopy. The ^{55}Mn , ^{59}Co , and ^1H spectra were recorded using a General Electric GN 300 spectrometer equipped with an 89-mm Oxford magnet. The measurements employed a high-pressure Be–Cu NMR probe with an internal toroid detector that was designed in-house and has been previously described.^{7,8} The pressure within the NMR cell was measured with a strain-gage transducer (Omega, Model PX302-5KGV). The strain-gage pressure transducer was calibrated against an accurate test gage, ± 15 at 5000 psi Model PGT-60B-5000 from Omega Engineering. The temperature was measured with a copper–constantan thermocouple that was mounted within the furnace, which is in direct thermal contact with the Be–Cu NMR cell. The temperature was controlled by the standard circuitry of the GE NMR spectrometer utilizing the copper–constantan thermocouple. For comparison, the temperature measurements at the NMR console were found to agree to within ± 0.1 °C, over the range 25–175 °C, with an independent determination made by placing a chromel–alumel thermocouple inside the pressure vessel. The chemical shifts observed in supercritical carbon dioxide (^{55}Mn NMR: $\text{Mn}_2(\text{CO})_{10}$, δ –2320 ppm; $\text{HMn}(\text{CO})_5$, δ –2560 ppm; $\text{MnCo}(\text{CO})_5$, δ –1820 ppm. ^{59}Co NMR: $\text{Co}_2(\text{CO})_8$, δ –2200 ppm; $\text{HCo}(\text{CO})_4$, δ –3000 ppm; $\text{MnCo}(\text{CO})_5$, δ –2830 ppm. ^1H NMR: H_2 , δ 4.45 ppm; $\text{HMn}(\text{CO})_5$, δ –7.84 ppm; $\text{HCo}(\text{CO})_4$, δ –11.70 ppm) compare favorably with literature values,⁹ for these compounds reported in organic solvents.

Materials. Dimanganese decacarbonyl, from Strem Chemical, was stored cold and used without further purification. Hydrogen from Matheson Gas Products (99.99% prepurified) was used as the primary concentration standard in the ^1H NMR integrations. Carbon monoxide, which was required to stabilize the solutions of the metal carbonyls, was also obtained from Matheson Gas Products (99.5%). The reactions were conducted in supercritical carbon dioxide, from AGA Specialty Gas (99.99%, <20 ppm O_2), at a fluid density of approximately 0.5 g/mL, which was obtained by injecting liquified carbon dioxide into the NMR cell with a high-pressure syringe pump (from ISCO) until the total pressure of the system increased by 82 atm at 34 °C. This latter value was chosen to be safely above the critical parameters¹⁰ for carbon dioxide, 80.0 atm at 31.2 °C, to provide a single homogeneous fluid phase within the NMR cell with a fluid density near the critical value for carbon dioxide. The supercritical fluid density was constant throughout the temperature range investigated, because the NMR pressure probe is a closed container. The carbon dioxide solvent was always the last component to be added to the NMR cell so that the residual volume of the

- (1) (a) Halpern, J. *Adv. Catal.* **1959**, *11*, 301–381. (b) Halpern, J. J. *Organomet. Chem.* **1980**, *200*, 133–144. (c) James, B. R. *Homogeneous Hydrogenation*; Wiley: New York, 1982; pp 204–208. (d) Yamamoto, A. *Organotransition Metal Chemistry*; Wiley-Interscience: New York, 1986; Chapter 4.
- (2) (a) Ungváry, F.; Markó, L. *J. Organomet. Chem.* **1969**, *20*, 205–209. (b) Alemdaroglu, N. H.; Penninger, J. M. L.; Oltay, E. *Monatsh. Chem.* **1976**, *107*, 1043–1053. (c) Tannenbaum, R. Ph.D. Dissertation, Dissertation ETH No. 6970, Swiss Federal Institute of Technology, Zurich, Switzerland. (d) Iwanaga, R. *Bull. Chem. Soc. Jpn.* **1962**, *35*, 774–778.
- (3) (a) Wegman, R. W.; Brown, T. L. *J. Am. Chem. Soc.* **1980**, *102*, 2494–2495. (b) Roth, J. A.; Orchin, M. *J. Organomet. Chem.* **1979**, *182*, 299–311. (c) Clark, A. C.; Terapane, J. F.; Orchin, M. *J. Org. Chem.* **1974**, *39*, 2405–2407. (d) Ungváry, F. *J. Organomet. Chem.* **1972**, *36*, 363–370.
- (4) Rathke, J. W.; Klingler, R. J.; Krause, T. R. Submitted for publication.
- (5) (a) Pino, P.; Piacenti, F.; Bianchi, M. In *Organic Synthesis via Metal Carbonyls*; Wender, I.; Pino, P., Eds.; Wiley: New York, 1977; Vol. 2, Chapter 2. (b) Paulik, F. E. *Catal. Rev.* **1972**, *6*, 49–84. (c) Orchin, M.; Rupilius, W. *Catal. Rev.* **1972**, *6*, 85–131. (d) Prueett, R. L. *Advances in Organometallic Chemistry*; Stone, F. G. A., West, R., Eds.; Academic Press: New York, 1979; Vol. 17, pp 1–60.
- (6) (a) Sweany, R. L.; Halpern, J. *J. Am. Chem. Soc.* **1977**, *99*, 8335–8337. (b) Halpern, J. *Pure Appl. Chem.* **1986**, *58*, 575–584. (c) Sweany, R.; Butler, S. C.; Halpern, J. *J. Organomet. Chem.* **1981**, *213*, 487–492. (d) Bullock, R. M.; Samsel, E. G. *J. Am. Chem. Soc.* **1987**, *109*, 6542–6544. (e) Baird, M. C. *Chem. Rev.* **1988**, *88*, 1217–1227. (f) Brown, T. L. Atom Transfer Reactions and Radical Chain Processes Involving Atom Transfer. In *Organometallic Radical Processes*; Troglér, W., Ed.; Elsevier: Lucerne, Switzerland, 1990.
- (7) (a) Rathke, J. W. *J. Magn. Reson.* **1989**, *85*, 150–155.
- (8) (a) Rathke, J. W.; Klingler, R. J.; Krause, T. R. *Organometallics* **1991**, *10*, 1350–1355. (b) Klingler, R. J.; Rathke, J. W. *Prog. Inorg. Chem.* **1991**, *39*, 131.

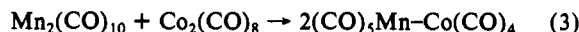
- (9) (a) Kidd, R. G.; Goodfellow, R. J. The Transition elements. In *NMR and the Periodic Table*; Harris, R. K., Mann, B. E., Eds.; Academic Press: New York, 1978, pp 219 and 235. (b) Jesson, J. P. Stereochemistry and Stereochemical Nonrigidity in Transition Metal Hydrides. In *Transition Metal Hydrides*; Muetterties, E. L., Ed.; Marcel Dekker: New York, 1971; pp 109 and 115.
- (10) McHugh, M.; Krukonis, U. *Supercritical Fluid Extraction*; Butterworths: Stoneham, MA, 1986.

capillary manifold tubing (0.254-mm i.d.) would be filled with liquified carbon dioxide, during the NMR measurements.

Concentration Data. The primary method for calculating the concentration data for the equilibrium of eq 2 was based on the relative peak areas for all the manganese-containing species observed in the ^{55}Mn NMR spectra and total mass balance in manganese. The initial dimanganese decacarbonyl concentrations were calculated from the weighed quantity of $\text{Mn}_2(\text{CO})_{10}$ and the free internal volume of the NMR pressure vessel. For comparison purpose, the $\text{HMn}(\text{CO})_5$ concentrations were alternatively calculated from the area ratio of the hydride resonance relative to the H_2 peak in the ^1H NMR spectra. Analogous calculations were performed by the two methods for the $\text{HCo}(\text{CO})_4$ and $\text{Co}_2(\text{CO})_8$ concentrations based on the ^{59}Co and ^1H NMR spectra. The second integration method, which is based on the hydrogen concentration as an internal integration standard, was employed to confirm that all the loaded metal carbonyls had dissolved in the supercritical carbon dioxide solvent. The required hydrogen concentrations, in M, were calculated on the basis of the ideal gas law and the measured temperature and pressure. The hydrogen concentration was effectively constant throughout the run, because the amount consumed by the reactions of eqs 1 and 2 was less than 5% of the initial loading and additional hydrogen-containing products, such as water from the reverse water-gas shift reaction or hydrocarbons from carbon monoxide hydrogenation, were not observed to any appreciable extent in the ^1H NMR spectra. It is noted that small quantities of water located at $\delta = 0.88$ ppm in the ^1H NMR spectra were produced in the initial stage of the reaction, presumably from the reverse water-gas shift reaction. The water levels rapidly leveled out in the concentration range 0.010–0.028 M, depending on the reaction temperature. In no case did the water byproduct consume more than 2% of the initial hydrogen loading of 1.37 M. These small equilibrium water concentrations are consistent with the unfavorable free energy change for the reverse water-gas shift reaction and the fact that the experiments were conducted under 500–850 psi of carbon monoxide. Similarly, the rate of carbon monoxide hydrogenation is expected to be slow with $\text{Mn}_2(\text{CO})_{10}$ and $\text{Co}_2(\text{CO})_8$ catalysts,^{9b,11a} under these reaction conditions, and consistently, there was no appreciable evidence for the production of methanol or saturated hydrocarbons in either the ^1H or the ^{13}C NMR spectra on the time scale of the reactions in eqs 1 and 2. Thus, at 220 °C the equilibrium of eq 2 is established in less time than it takes to equilibrate the temperature and adjust the magnet homogeneity, ≈ 30 min. In contrast, the production of methanol through carbon monoxide hydrogenation with a $\text{Mn}_2(\text{CO})_{10}$ catalyst is slow^{11a} even at 240 °C, with a pseudo-first-order rate constant of $1.3 \times 10^{-5} \text{ s}^{-1}$. It is of further note that the observed line widths for both the water and hydrogen remained invariant, 10 ± 2 Hz, in the ^1H NMR spectra even under conditions where the hydride resonances in $\text{HMn}(\text{CO})_5$ and $\text{HCo}(\text{CO})_4$ had merged. Therefore, dynamic processes involving water or hydrogen are slower or, at least, less extensive than the process(es) that equilibrates the hydride moieties. Consistent with earlier observations,^{9a} there were no observable resonances in the region expected for formate complexes in either the ^1H or the ^{13}C NMR spectra and the resonance for the carbon dioxide solvent remained sharp up to 220 °C in the ^{13}C spectra. Thus, there is no evidence for carbon dioxide complex formation or other species that might interfere with the equilibrium measurements of eqs 1 and 2.

Results

The direct hydrogenation of dimanganese decacarbonyl (eq 2) is observable¹¹ under 34 atm of hydrogen at temperatures in excess of 165 °C. However, the manganese system of eq 2 is significantly slower than the cobalt analogue of eq 1. Therefore, $\text{Co}_2(\text{CO})_8$ was investigated as a potential catalyst for the hydrogenation of dimanganese decacarbonyl in an attempt to extend the temperature range over which it is possible to measure the equilibrium constant for the reaction in eq 2. The reaction in the mixed-metal system proceeds smoothly, resulting in the formation of both relevant metal hydrides, $\text{HMn}(\text{CO})_5$ and $\text{HCo}(\text{CO})_4$, as well as the mixed dimer (eq 3), and was conveniently followed by ^{59}Co and ^{55}Mn



NMR spectroscopy as demonstrated in Figure 1. Thus, with the addition of the $\text{Co}_2(\text{CO})_8$ promoter it became feasible to follow $\text{HMn}(\text{CO})_5$ production, in an experimentally reasonable time frame, for temperatures down to 80 °C. For example, the data in Figure 2 demonstrate that it requires approximately 48 h for $\text{HMn}(\text{CO})_5$ to reach its equilibrium value of 2.8 mM, under 34

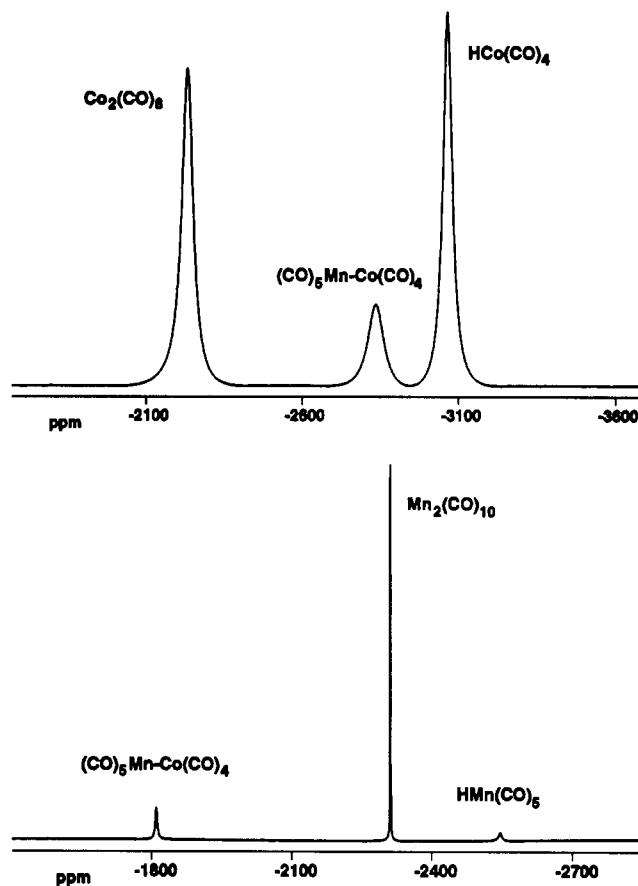


Figure 1. ^{59}Co and ^{55}Mn NMR spectra, upper and lower traces, for the reaction of $\text{Mn}_2(\text{CO})_{10}$, 0.015 M, and $\text{Co}_2(\text{CO})_8$, 0.018 M, at 100 °C under 34 atm of H_2 and 34 atm of CO in supercritical carbon dioxide ($d = 0.5 \text{ g/mL}$).

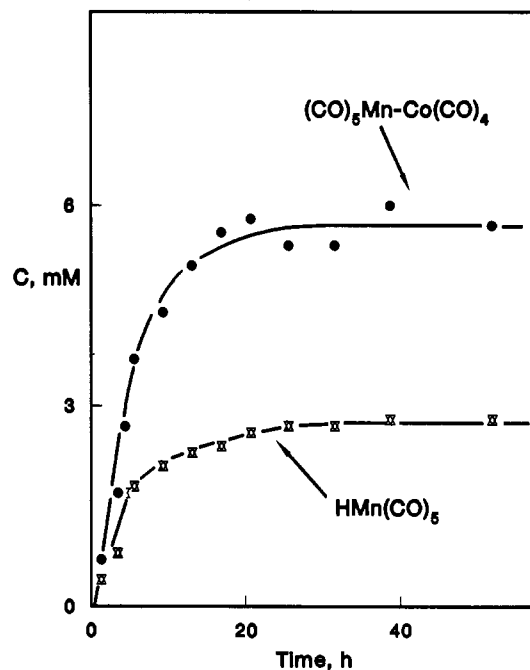


Figure 2. Manganese products in the $\text{Co}_2(\text{CO})_8$ -promoted hydrogenation of $\text{Mn}_2(\text{CO})_{10}$. Conditions are as in Figure 1.

atm of H_2 at 100 °C. The data in Figure 2 yield a linear pseudo-first-order rate plot for the approach to equilibrium with a half-life of 6.2 h. For comparison, the background hydrogenation of $\text{Mn}_2(\text{CO})_{10}$ in the absence of the $\text{Co}_2(\text{CO})_8$ promoter was followed for 144 h at 100 °C, yielding an estimate for the half-life of ≈ 2400 h. Thus, the $\text{Co}_2(\text{CO})_8$ promoter leads to a rate en-

(11) (a) Rathke, J. W.; Feder, H. M. *J. Am. Chem. Soc.* 1978, 100, 3623.
(b) Hieber, W.; Wagner, G. *Z. Naturforsch.* 1958, B13, 339–347.

Table I. Hydride Concentrations in the Slow-Exchange Limit^a

temp, °C	obs ^b	[HMn(CO) ₅], mM		[HCo(CO) ₄], mM	
		⁵⁵ Mn data ^c	¹ H data ^d	⁵⁹ Co data ^c	¹ H data ^d
100	13	2.8 (0.2)	2.3 (0.4)	14.5 (0.1)	14.6 (0.8)
110	8	3.3 (0.2)	3.7 (0.6)	15.4 (0.1)	14.8 (0.6)
120	8	3.9 (0.1)	3.9 (1)	15.7 (0.2)	16.4 (1)

^a For the reaction of Mn₂(CO)₁₀, 0.015 M, and Co₂(CO)₈, 0.018 M, with [H₂] = [CO] = 1.37 M, in supercritical carbon dioxide, *d* = 0.5 g/mL. ^b The number of spectra which were averaged, standard deviation in parentheses. ^c Based on the relative ratios of all the metal containing species in the NMR spectrum and the initial dimer concentration. ^d Based on the ratio of the hydride to the H₂ standard in the ¹H NMR spectrum.

hancement of approximately 2 orders of magnitude in the hydrogenation of Mn₂(CO)₁₀.

The ⁵⁹Co and ⁵⁵Mn NMR spectra were used as the primary analytical technique for measuring the concentrations of the organometallic species, as described in the Experimental Section. In addition, the ¹H NMR spectra were used to provide an independent check on the hydride concentrations, by measuring the ratio of the hydride resonances to the H₂, which was known to be present at 1.37 M. The comparative results for these two methods are summarized in Table I, for the temperature range 100–120 °C.

At higher temperatures, the hydride resonances in the ¹H NMR spectra for HMn(CO)₅ and HCo(CO)₄ merged, indicating a process exists which exchanges the hydride moiety. Recently, Markó et al. have investigated¹² the hydride ligand transfer reaction between a series of metal carbonyl hydrides with a number of homo- and heterometal carbonyl dimers by infrared spectroscopy. Indeed, they found that the hydride moiety is transferred within the manganese/cobalt system under mild reaction conditions, 0–40 °C for the reaction in eq 4. It is not possible to



obtain independent HMn(CO)₅ and HCo(CO)₄ concentrations from the ¹H NMR data in the presence of this exchange process at temperatures much in excess of 120 °C. Therefore, the proton spectra could not be utilized as the primary method to determine the hydride concentrations at all the temperatures investigated. Fortunately, the ⁵⁵Mn spectra exhibited sharp well-resolved resonances up to 220 °C and were well suited to measure the HMn(CO)₅ and Mn₂(CO)₁₀ concentrations. It is noted that the resonances for HCo(CO)₄ and Co₂(CO)₈ do merge in the ⁵⁹Co NMR spectra for temperatures near¹³ 200 °C. These exchange processes, as well as the mechanistic interpretation of the promotional effect of Co₂(CO)₈ on the hydrogenation of Mn₂(CO)₁₀, will be addressed in greater detail at a later time.

It is possible to use the ¹H NMR data as a check on the total hydride concentration, in the presence of the exchange process in eq 4. Thus, at temperatures in excess of approximately 160 °C, the combined hydride resonance for HMn(CO)₅ and HCo(CO)₄ in the ¹H NMR spectra is sufficiently sharp that it may be integrated to provide a total hydride concentration, column 6 in Table II. This value compares with the hydride concentrations independently calculated from the ⁵⁵Mn and ⁵⁹Co NMR data,¹⁴ columns 3 and 4 of Table II, which are summed in column 5.

(12) Kovács, I.; Sisak, A.; Ungváry, F.; Markó, L. *Organometallics* **1989**, *8*, 1873–1877.

(13) Unpublished results.

(14) At the temperatures listed in Table II, the error in the HCo(CO)₄ concentrations from the ⁵⁹Co NMR spectra is undoubtedly larger than that reflected in the standard deviation of the individual observations, because the resonances for CoMn(CO)₉ and HCo(CO)₄ begin to overlap as the line width of the HCo(CO)₄ peak increases; compare Figure 1. It is further noted that the overlap in the ⁵⁹Co spectra does not directly effect the calculation of the manganese concentration data for the process in eq 2. Similarly, the cobalt equilibrium in eq 1 can be accurately measured⁴ in the absence of CoMn(CO)₉.

Table II. Hydride Concentrations in the Fast-Exchange Limit^a

temp, °C	obs ^b	[HMn(CO) ₅], ^c mM	[HCo(CO) ₄], ^c mM	Σ, ^d mM	[hydride], ^e mM
170	5	7.8 (0.8)	14.5 (0.3)	22 (1)	16.5 (0.7)
180	5	8.3 (0.6)	13.0 (0.4)	21 (1)	18.2 (0.7)
190	5	9.5 (0.5)	10.7 (0.3)	20 (1)	20 (2)

^a Conditions in Table I. ^b The number of spectra which were averaged, standard deviation in parentheses. ^c Based on the relative ratios of all the metal containing species in the NMR spectrum and the initial dimer concentration. ^d Sum of the hydride concentrations obtained from the metal NMR spectra in columns 3 and 4. ^e Based on the ratio of the merged hydride resonance to the H₂ standard in the ¹H NMR spectrum.

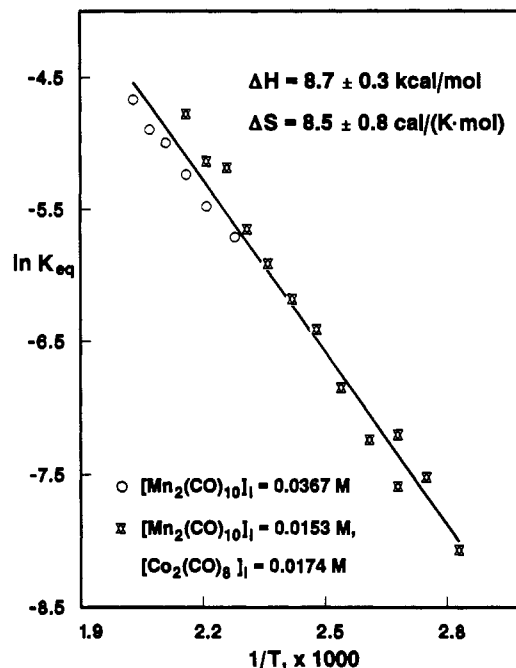


Figure 3. van't Hoff plot for the hydrogenation of Mn₂(CO)₁₀, with conditions as in Table III.

Discussion

Previous results on the hydrogenation of Co₂(CO)₈ (eq 1) have demonstrated that thermodynamic parameters are obtained in supercritical carbon dioxide⁴ similar to those reported in *n*-heptane² solvent. In addition, the net rate of aldehyde production and the steady-state HCo(CO)₄ and RC(O)Co(CO)₄ concentrations are also quite similar for the hydroformylation reaction conducted in supercritical carbon dioxide^{8a} compared with results in methylcyclohexane¹⁵ solvent. These observations indicate that, within the cobalt-catalyzed hydroformylation system, neither the thermodynamic nor the kinetic properties for the hydrogenation of eq 1 exhibit unusual solvent effects in supercritical carbon dioxide. However, the supercritical fluid reaction medium does have distinct experimental advantages for the NMR studies. Thus, the natural NMR line widths for quadrupolar nuclei can be 1 order of magnitude sharper in supercritical solvents,^{8,16a} due to the lower viscosity of the supercritical fluid, compared to that of organic solvents.¹⁰ Furthermore, it is unnecessary to measure gas–liquid partition coefficients in the single-phase supercritical carbon dioxide fluid, while the design of the pressure vessel is simplified, because it is no longer necessary to include a mechanical means to effect mixing^{16b} in a homogeneous supercritical fluid medium.

The hydrogenation of Mn₂(CO)₁₀ (eq 2) has been investigated in supercritical carbon dioxide both with and without the addition of a Co₂(CO)₈ promoter. The resultant equilibrium constant data are given in the van't Hoff plot of Figure 3. The extended

(15) Mirbach, M. F. *J. Organomet. Chem.* **1984**, *265*, 205–213.

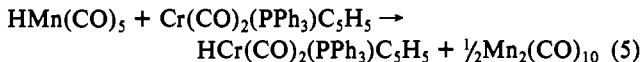
(16) (a) Robert, J. M.; Evilia, R. F. *J. Am. Chem. Soc.* **1985**, *107*, 3733–3735. (b) Vander Velde, D. G.; Jonas, J. J. *Magn. Reson.* **1987**, *71*, 480–484.

Table III. Thermodynamic Parameters for the Hydrogenation of $\text{Mn}_2(\text{CO})_{10}$

system	ΔH , kcal	ΔS , ^a cal/(mol·K)
unpromoted ^b	8.3 ± 0.3	7.5 ± 0.7
$\text{Co}_2(\text{CO})_8$ promoted ^c	9.7 ± 0.4	11.2 ± 0.9
combined data	8.7 ± 0.3	8.5 ± 0.8

^a Standard state for H_2 is M. ^b For the reaction of $\text{Mn}_2(\text{CO})_{10}$, 0.037 M, with $[\text{H}_2] = 1.43$ M and $[\text{CO}] = 0.29$ M, in supercritical carbon dioxide, $d = 0.5$ g/mL. ^c For the reaction of $\text{Mn}_2(\text{CO})_{10}$, 0.015 M, and $\text{Co}_2(\text{CO})_8$, 0.018 M, with $[\text{H}_2] = [\text{CO}] = 1.37$ M, in supercritical carbon dioxide, $d = 0.5$ g/mL.

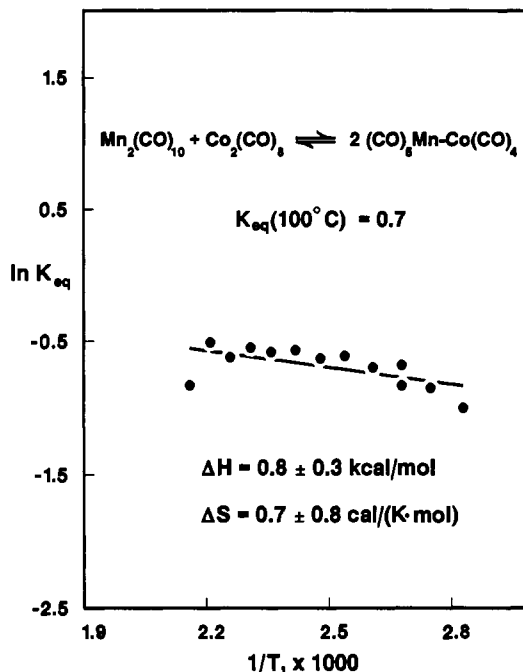
temperature range accessible to the hydrogenation reaction in the presence of the $\text{Co}_2(\text{CO})_8$ promoter is readily apparent in Figure 3. The resultant van't Hoff plot yields the standard enthalpy and entropy change for the reaction in eq 2 from the slope and intercept, respectively. The results are summarized in Table III. There does not appear to be a statistically significant difference between the results obtained with the $\text{Co}_2(\text{CO})_8$ promoter, row 2 of Table III, and the unpromoted reaction, row 1, because the standard deviations for the individual data sets nearly overlap with those from the combined data set, row 3. The standard enthalpy change for the hydrogenation of $\text{Mn}_2(\text{CO})_{10}$ in column 2 of Table III is reasonably consistent with a recent determination, 4.0 ± 2.4 kcal/mol, which was measured in toluene solution, based on the enthalpy change for the hydrogen atom transfer reaction in eq 5 and an application of Hess's law.¹⁷ As a further check on



the data, it is noted that the standard entropy change thus obtained for the gas-phase hydrogenation reaction in eq 2, column 3 of Table III, compares favorably to the value, $+4.4 \pm 0.5$ cal/(mol·K), previously obtained⁴ for the analogous hydrogenation of eq 1. Furthermore, Ungváry and Markó have obtained 4.4 cal/(mol·K) for the cobalt system of eq 1, although it is noted that this latter value was measured in *n*-heptane solvent and may not be directly comparable to the gas-phase values obtained in supercritical carbon dioxide.

The equilibrium constants are consistently lower for the manganese hydrogenation of eq 2 than the cobalt hydrogenation of eq 1. This is readily apparent in the spectra of Figure 1, where the ratio of $\text{HCo}(\text{CO})_4$ to $\text{Co}_2(\text{CO})_8$ is significantly larger than the analogous ratio of $\text{HMn}(\text{CO})_5$ to $\text{Mn}_2(\text{CO})_{10}$ under the same reaction conditions. The more favorable equilibrium constants for the hydrogenation of $\text{Co}_2(\text{CO})_8$ compared to $\text{Mn}_2(\text{CO})_{10}$ are a result of the more favorable enthalpy of hydrogenation⁴ for $\text{Co}_2(\text{CO})_8$ in eq 1, $+4.7 \pm 0.2$ kcal, relative to the value for the manganese system, eq 2 and column 2 of Table III. It is further seen that the absolute difference between the cobalt and manganese systems of eqs 1 and 2 is not very large in comparison to the magnitude of the BDE for the bonds formed and broken during the reaction (H_2 , 104 kcal; H-M, ≈ 70 kcal; M-M, ≈ 40 kcal). Thus, the difference in enthalpy between the two systems is $\Delta H_{\text{eq}2} - \Delta H_{\text{eq}1} = 4.0$ kcal, while at 150 °C the difference in the entropy terms is only $(T\Delta S)_{\text{eq}2} - (T\Delta S)_{\text{eq}1} = 1.7$ kcal.

Recently, the H-Mn BDE value of 68 kcal has been determined for $\text{HMn}(\text{CO})_5$ on the basis of electrochemical techniques in conjunction with acidity measurements,¹⁸ although lower estimates exist.¹⁹ Similarly, the Mn-Mn BDE for $\text{Mn}_2(\text{CO})_{10}$ has been investigated by a variety of techniques,²³ yielding a disappointingly

**Figure 4.** van't Hoff plot for the redistribution reaction between $\text{Mn}_2(\text{CO})_{10}$ and $\text{Co}_2(\text{CO})_8$, with conditions as in Table III.

large range of values from 20 to 40 kcal. However, the most recent determinations^{23,24} seem to favor the high end of this range, 38 ± 5 kcal. The determination of the standard enthalpy change for the hydrogenation of $\text{Mn}_2(\text{CO})_{10}$ in eq 2 now allows an independent comparison to be made between these BDE values for the Mn-Mn and Mn-H bonds. The resultant calculation using a BDE of 104 kcal for H_2 predicts the enthalpy of hydrogenation of $\text{Mn}_2(\text{CO})_{10}$ in eq 2 to be 6 ± 5 kcal, which compares favorably with the results in column 2 of Table III.

The mixed-dimer equilibrium data of Figure 4 indicate that the heterobimetallic bond formation process in eq 3 is nearly thermal neutral. None of the equilibrium constants differ substantially from unity over the temperature range of 80–190 °C. The data suggest that there is little ionic character to the Mn-Co bond in $\text{Mn}(\text{CO})_5\text{-Co}(\text{CO})_4$.

In contrast to the $\text{Mn}_2(\text{CO})_{10}$ system, the results for $\text{Co}_2(\text{CO})_8$ are not as well defined. Thus, the difference in the enthalpy of hydrogenation between eqs 1 and 2 is only 4 kcal, while the reported¹⁸ H-Co and H-Mn BDE differ by 1 kcal. These results imply that the Co-Co BDE differs, at most, from the Mn-Mn BDE by 6 kcal. Yet, the ⁵⁹Co NMR spectra exhibit a facile exchange process(es)⁴ at 200 °C that equilibrates the cobalt centers in $\text{HCo}(\text{CO})_4$ and $\text{Co}_2(\text{CO})_8$, while the line widths in the analogous ⁵⁵Mn spectra remain sharp up to 220 °C. Indeed, the ⁵⁹Co NMR resonance for $\text{Co}_2(\text{CO})_8$ broadens¹³ (reversibly as an exponential function of reciprocal temperature) even in the absence of H_2 , in a manner reminiscent of the reversible ¹H NMR spectral changes²⁵ for the $\text{Cp}_2\text{Cr}_2(\text{CO})_6$ system, which has a relatively weak Cr-Cr bond.^{27b} In addition, the existing van't Hoff analysis²⁶ of the equilibrium between $\text{Co}_2(\text{CO})_8$ and $\text{Co}(\text{CO})_4$ also yields

(17) Kiss, G.; Nolan, S. P.; Hoff, C. D. Private communication.

(18) (a) Tilsset, M.; Parker, V. D. *J. Am. Chem. Soc.* **1989**, *111*, 6711–6717. (b) Tilsset, M.; Parker, V. D. *J. Am. Chem. Soc.* **1990**, *112*, 2843.(19) Metal-hydride BDE values have recently been reviewed by an established authority in the field,²⁰ where it has been noted that other estimates exist for the H-Mn BDE based on the kinetics of hydrogen atom transfer,²¹ 63 kcal, and mass spectrometric appearance potentials,²² 60 kcal.

(20) Eisenberg, D. C.; Norton, J. R. Private communication.

(21) (a) Billmers, R.; Griffith, L. L.; Stein, S. E. *J. Phys. Chem.* **1986**, *90*, 517–523.(22) Miller, A. E.; Kawamura, A. R. *J. Am. Chem. Soc.* **1990**, *112*, 457–458.(23) Martinho Simões, J. A.; Beauchamp, J. L. *Chem. Rev.* **1990**, *90*, 629.(24) (a) Goodman, J. L.; Peters, K. S.; Vaida, V. *Organometallics* **1986**, *5*, 815–816. (b) Pugh, J. R.; Meyer, T. J. *J. Am. Chem. Soc.* **1988**, *110*, 8245–8246. (c) Martinho Simões, J. A.; Schultz, J. C.; Beauchamp, J. L. *Organometallics* **1985**, *4*, 1238–1242.(25) Adams, R. D.; Collins, D. E.; Cotton, F. A. *J. Am. Chem. Soc.* **1978**, *96*, 749–754.(26) (a) Bidinosti, D. R.; McIntyre, N. S. *J. Chem. Soc., Chem. Commun.* **1967**, 1. (b) Bidinosti, D. R.; McIntyre, N. S. *Can. J. Chem.* **1970**, *48*, 593–597.(27) (a) Landrum, J. T.; Hoff, C. D. *J. Organomet. Chem.* **1985**, *282*, 215–224. (b) McLain, S. J. *J. Am. Chem. Soc.* **1988**, *110*, 643–644. (c) Jaeger, T. J.; Baird, M. C. *Organometallics* **1988**, *7*, 2074–2076. (d) Cooley, N. A.; Watson, K. A.; Fortier, S.; Baird, M. C. *Organometallics* **1986**, *5*, 2563–2565.

a low BDE of 15 kcal. Further discussion of the Co-Co BDE value must await a complete analysis of the variable-temperature NMR spectrum of the $\text{Co}_2(\text{CO})_8/\text{Mn}_2(\text{CO})_{10}/\text{H}_2$ system, as well as that for similar mixed-metal systems with stable metal-centered radicals, whose thermodynamics are unequivocally established. A prime candidate in this regard is the $[\text{Cp}^*\text{Cr}(\text{CO})_3]_2/\text{HCr}(\text{CO})_3\text{Cp}^*$ ($\text{Cp}^* = \eta\text{-C}_5\text{Me}_5$) system,²⁷ because the $\text{Cp}^*\text{Cr}(\text{CO})_3$ radical exhibits reversible electrochemistry¹⁸ and is sufficiently stable that the enthalpy of hydrogenation of the radical has been directly measured by calorimetry.²⁸

Acknowledgment. We thank Professors J. Norton and C. Hoff for useful discussions and providing preprints of their work. Similar appreciation is extended to Professor J. Halpern for helpful discussions. Support for this work was provided by the Office of Basic Energy Sciences, Division of Chemical Sciences, U.S. Department of Energy, under Contract W-31-109-ENG-38.

(28) Kiss, G.; Zhang, K.; Mukerjee, S. L.; Hoff, C. D. *J. Am. Chem. Soc.* **1990**, *112*, 5657-5658.

Contribution from the Guelph-Waterloo Centre for Graduate Work in Chemistry, Department of Chemistry and Biochemistry, University of Guelph, Guelph, Ontario, Canada N1G 2W1

Electron-Transfer Reactions of Cobalt(III) Complexes Possessing Oxsulfur Ligands

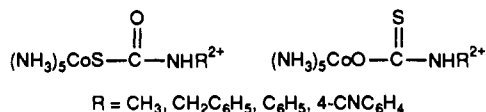
Michael D. Johnson and Robert J. Balahura*

Received August 22, 1991

The kinetics of the chromium(II) reduction of a series of cobalt(III) complexes possessing an oxsulfur bridging ligand have been measured. At 25 °C, $I = 1.0 \text{ M}$ (LiClO_4) the second order rate constants for the pentaamminecobalt(III) complexes of SO_3^{2-} , $\text{C}_6\text{H}_5\text{SO}_2^-$, and $\text{S}_2\text{O}_5^{2-}$ are $4.7 (\pm 0.3) \times 10^3$, $5.3 (\pm 0.1) \times 10^3$, and $2.1 (\pm 0.1) \times 10^4 \text{ M}^{-1} \text{ s}^{-1}$, respectively. The reduction of *trans*- $(\text{NH}_3)_4\text{Co}(\text{OH}_2)\text{SO}_3^+$ by chromium(II) has also been studied and yields a rate constant of $1.1 (\pm 0.1) \times 10^5 \text{ M}^{-1} \text{ s}^{-1}$ at 25 °C, $I = 1.0 \text{ M}$ (LiClO_4). The value of $18.6 \text{ M}^{-1} \text{ s}^{-1}$ for the rate constant for chromium(II) reduction of the sulfite complex reported in 1965 is now seen to be incorrect. The data are discussed in terms of a ground-state trans effect induced by the coordinated sulfur atom.

Introduction

A recent study of the reduction of the linkage isomers of the monothiocarbamate complexes



by chromium(II) has shown that the unusually rapid reduction of the S-bonded complexes is mainly due to a ground-state structural trans effect (STE) in the oxidant.¹ The S-bonded sulfite complex $(\text{NH}_3)_5\text{CoSO}_3^+$ has one of the largest known STEs (0.089 \AA^2) and its rate of reduction by chromium(II) has been reported as $18.6 \text{ M}^{-1} \text{ s}^{-1}$ (25 °C).³ This value is approximately 4 orders of magnitude less than that predicted on the basis of the STE.⁴ The sulfite complex can only be prepared and purified in solutions containing free ammonia,⁵ and it reacts rapidly in acidic medium to form *trans*- $(\text{NH}_3)_4\text{Co}(\text{OH}_2)\text{SO}_3^+$. The latter complex also undergoes internal redox decomposition.⁶ Due to these complications and our recent findings, we have reinvestigated the reaction of $(\text{NH}_3)_5\text{CoSO}_3^+$ with Cr^{2+} . We also report kinetic data for the reduction of $(\text{NH}_3)_5\text{CoS}_2\text{O}_5^+$, $(\text{NH}_3)_5\text{CoSO}_2\text{C}_6\text{H}_5^{2+}$, and *trans*- $(\text{NH}_3)_4\text{Co}(\text{OH}_2)(\text{SO}_3)^+$ by Cr^{2+} .

Experimental Section

Materials. $[\text{Co}(\text{NH}_3)_5\text{SO}_3]\text{ClO}_4$,⁷ $[\text{Co}(\text{NH}_3)_5\text{S}_2\text{O}_5]\text{ClO}_4$,⁸ and $[\text{Co}(\text{NH}_3)_5(\text{benzenesulfonato})]\text{ClO}_4$ were prepared according to literature

methods. *trans*- $(\text{NH}_3)_4\text{Co}(\text{OH}_2)\text{SO}_3^+$ was prepared by dissolving $\text{Co}(\text{NH}_3)_5\text{SO}_3^+$ in water. Chromium(II) solutions were obtained via reduction of stock chromium(III) perchlorate using zinc amalgam. Concentrations were standardized as previously described.¹

Kinetics. Reaction rates were measured using a Durrum D110 stopped-flow spectrophotometer interfaced with a computerized data acquisition system. Rate constants were obtained from processing of the raw data utilizing programs developed by the OLIS Corp. (Jefferson, GA). All rate constants are averages of three runs and are precise to at least 10%.

Ionic strength was maintained using lithium perchlorate and perchloric acid stock solution. These solutions were standardized as described previously.¹ Due to the oxygen sensitivity of chromium(II), all reactions were carried out under a blanket of argon using standard syringe techniques.

Results and Discussion

When $[(\text{NH}_3)_5\text{CoSO}_3](\text{ClO}_4)$ is dissolved in neutral or acidic solution, the visible absorption spectrum gives a maximum at 472 nm ($\epsilon = 160 \text{ M}^{-1} \text{ cm}^{-1}$). The latter peak indicates the presence of *trans*- $(\text{NH}_3)_4\text{Co}(\text{OH}_2)\text{SO}_3^+$ formed by the rapid substitution of the ammonia trans to the sulfite group.⁶ The sulfitepentaamminecobalt(III) cation, however, persists in 0.10 M $\text{NH}_3(\text{aq})$ and gives a visible maximum at 456 nm ($\epsilon = 150 \text{ M}^{-1} \text{ cm}^{-1}$). If a solution of the sulfite complex in 0.10 M $\text{NH}_3(\text{aq})$ is mixed with 1.0 M $\text{HClO}_4(\text{aq})$ on a stopped-flow instrument, the formation of the *trans*-substituted complex is complete in approximately 2 min. The reaction can be conveniently observed at 472 nm where the expected increase in absorbance is significant. In the reduction studies all the acid was contained in the chromium(II) solutions which were then mixed with $(\text{NH}_3)_5\text{CoSO}_3^+$ in 0.10 M $\text{NH}_3(\text{aq})$. At 450-472 nm only an absorbance decrease was observed consistent with reduction of cobalt(III) to cobalt(II). More importantly, under these conditions, reduction of the sulfite complex was much faster (approximately 3 orders of magnitude) than the substitution reaction as observed above. The observed rate constants collected in this manner were first order in both complex

- Balahura, R. J.; Johnson, M. D.; Black, T. *Inorg. Chem.* **1989**, *28*, 3933.
- Elder, R. C.; Heeg, M.; Payne, M.; Trkula, M.; Deutsch, E. *Inorg. Chem.* **1978**, *17*, 431.
- Peters, D. E.; Fraser, R. T. M. *J. Am. Chem. Soc.* **1965**, *87*, 2758.
- Deutsch, E.; Root, M.; Nisco, D. *Adv. Inorg. Bioinorg. Mech.* **1982**, *1*, 269.
- Siebert, H.; Wittke, G. *Z. Anorg. Allg. Chem.* **1973**, *399*, 43.
- Thacker, M.; Scott, K.; Simpson, M.; Murray, R.; Higginson, W. J. *Chem. Soc., Dalton Trans.* **1974**, 647.
- Elder, R. C.; Trkula, M. *J. Am. Chem. Soc.* **1974**, *96*, 2635.
- Balahura, R. J.; Johnson, M. D. *Inorg. Chem.* **1988**, *27*, 3104.